Phase Transition in Epitaxial Bismuth Nanofilms

Feng He^{1,2}, Emily S. Walker³, Yongjian Zhou¹, Raul D. Montano¹, Seth R. Bank³ and Yaguo Wang^{1,2*}

- Department of Mechanical Engineering, The University of Texas at Austin, Austin, TX, 78712, USA
- 2. Texas Materials Institute, The University of Texas at Austin, Austin, TX, 78712, USA
- 3. Microelectronics Research Center and Department of Electrical and Computer Engineering, The University of Texas at Austin, Austin, TX, 78758, USA
- *Corresponding Author. Email: yaguo.wang@austin.utexas.edu

Abstract

Raman and coherent phonon spectroscopies were used to investigate the thickness dependent phononic properties of ultrathin single-crystal Bi films prepared with molecular beam epitaxy (MBE) on Si(111) substrates. The A_{1g} and E_g Raman peaks both disappeared in the Raman spectra of a 4 nm Bi film, indicating a complete transition from the low-symmetry A7 structure to the high-symmetry A17 structure. Coherent phonon signals of the A_{1g} mode also showed a strong dependence on film thickness, where thin samples (≤ 15 nm) exhibited lower phonon frequency and shorter phonon lifetimes than that of the thick samples (≥ 30 nm). This difference is attributed to a shallower energy potential barrier caused by both a permanent phase transition, which is determined by the film thickness, and a temporary structural transition by photo-excited carriers. Our results not only provide evidence of a phase transition from the A7 to the A17 structure with decreasing Bi film thickness, but also reveal the influence of this phase transition on phonon dynamics. Understanding these material performance traits will facilitate modern application of Bi thin films in novel electronic devices.

Bismuth, with a Peierls distortion structure ¹, has been extensively studied since the 1960s because of its unique atomic and electronic structures. The slight overlap between the conduction and valence bands makes it a semimetal with a low number of carriers, thus an exceptionally long electron mean free path at room temperature (~2 µm) ². In recent years, with the development of a suitable growth technique, high quality bismuth films can be obtained through molecular beam epitaxy (MBE). This innovation has attracted a renewed interest to investigate new physics in this prototype semimetal, such as ultrafast bond softening ³, exceptional surface-state spin and valley properties ^{4, 5}, semimetal-semiconductor (SM-SC) transition ^{6, 7}, superconductivity ², topological insulator states, 2D spintronic phenomena ⁸⁻¹¹, transient high-symmetry phase transformation ¹², and strong anharmonic scattering ^{13, 14}. All of these properties, combined with a negative real and small imaginary part of the dielectric constant and the strong inter-band transition, make the MBE-grown Bi thin film promising for application in inter-band plasmonics ¹⁵.

Usually, a bulk Bi crystal finds natural stability in an A7 structure with a Rhombohedral primitive cell containing two Bi atoms per cell, and an intrinsic crystal growth direction is along hexagonal (001). Some new phases were observed in the early stages of material growth with MBE, where the first several monolayers (ML) of Bismuth were contrived to adapt to the crystal structure of the substrate. Recently, Fang et al. found a temporary phase showing periodic regions when growing Bi on NbSe₂ substrate with MBE ¹⁶. Back in 2004, Nagao et al. conducted extensive studies to show that with a Si(111) substrate, the first four ML had a pseudocubic puckered 2D structure, similar to that of black phosphorus (BP) ^{17, 18}. This puckered structure could either be the real A17 structure (Fig. 1b), or the A7 structure along the {012} direction (Fig. 1c). Reflection high-energy electron diffraction (RHEED), which is generally used to monitor the crystal structure in-situ during an MBE growth, could not distinguish A17 from A7 {012} because they produce very similar diffraction patterns due to their same out-of-plane lattice constant ¹⁸. As Bi films grow thicker, they gradually transition to the conventional A7 (001) structure. The threshold for the number of ML for this transition to occur spans from 4 ML to 7 ML, the true value of which being dependant on the substrate temperature. The BP-like A17 structure possesses a cubic unit cell with only one atom per unit cell. Due to the fundamental differences between the A17 and A7 crystal structures, they may be distinguished through their phononic properties. When a crystal has two atoms per primitive cell, it has 6 phonon branches: 3 acoustic and 3 optical. For A7 Bi, the signature optical branches are the A_{1g} and E_g phonons, which polarize perpendicular & parallel to

the hexagonal (001) plane, as described in Fig. 2a. For the A17 structure, there are only 3 acoustic branches because of it containing one atom per primitive cell. As a result, no A_{1g} or E_g phonons can be observed in the A17 structure.

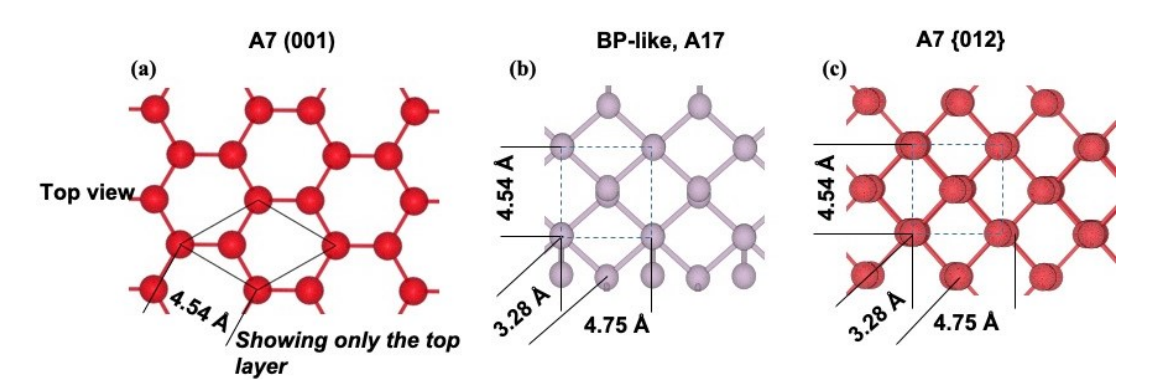


Figure 1 Schematics of bismuth crystal structures in top view: (a) A7 (rhombohedral) structure along hexagonal (001) direction; (b) A17 (pseudocubic, black-phosphorus) structure; and (c) A7 (rhombohedral) structure along hexagonal {012} direction. The A17 and A7 {012} structures share the same lattice constant and atomic density, therefore producing very similar diffraction pattern in the RHEED spectra.

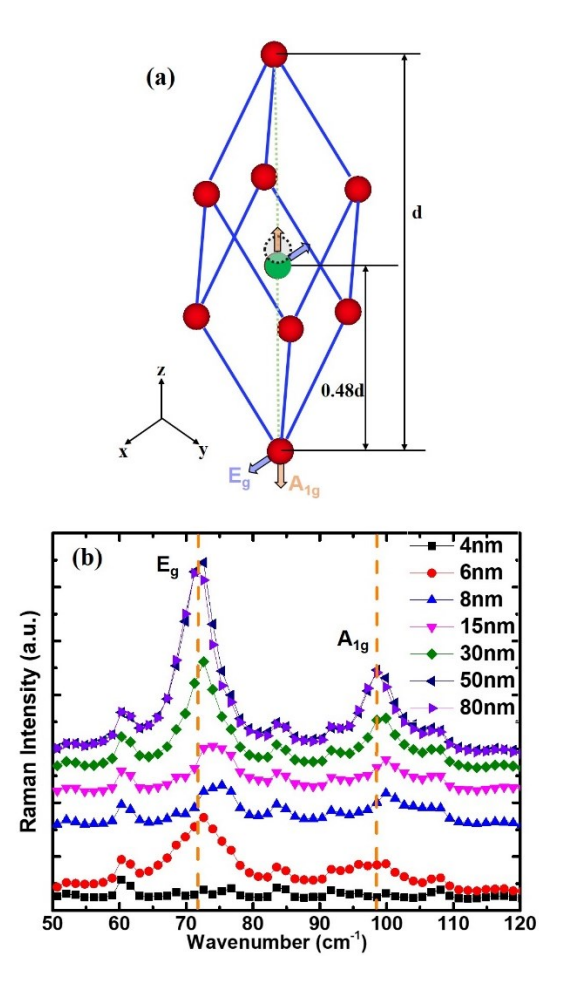


Figure 2 (a) Schematic diagram of the A_{1g} (longitudinal, orange arrow) and E_g (transverse, blue arrow) modes in an A7 rhombohedral unit cell. The coordinates are in the hexagonal indexing, i.e. z axis is hexagonal (001), corresponding to the (111) plane in rhombohedral indexing. At equilibrium, the Bi atom inside the unit cell (green atom) sits at (0.48:0.52) along the diagonal axis. The dashed circle marks the position of the center along the diagonal axis. (b) Raman spectra of Bi thin films ranging from 4 nm to 80 nm. The signature E_g and A_{1g} modes in 80 nm and 50 nm thin films are marked by orange vertical lines as references.

We performed Raman spectroscopy on the MBE synthesized Bi films on Si(111) varying from 4 nm to 80 nm (see Fig. S1 – S3) utilizing an inViaTM confocal Raman microscope (Renishaw) operating with 532 nm excitation. These results are shown in Fig. 2b, presenting several noteworthy features. Raman spectra of 80 nm and 50 nm totally overlap, indicating at this thickness range Bi films show bulk properties. When the material thickness decreases, both A_{1g} and E_g peaks shift to higher frequency with intensity decreases. This is usually attributed to the strain generated at Bi/Si interface due to lattice mismatch. The subsequent Raman spectra of 15

nm and 8 nm samples proved to be almost the same. At 6 nm, both A_{1g} and E_{g} peaks become much broader and shift a little bit back to a lower frequency. At 4 nm, both A_{1g} and E_{g} peaks suddenly disappear completely. Disappearance of both the A_{1g} and E_{g} peaks in a 4 nm thick film is a strong evidence of phase transition from an A7 to an A17 structure, considering the fact that A17 structure does not have any optical phonon branches. The complex features at 6 nm might come from the transition region from A7 to A17. With Raman Spectroscopy, we confirmed the phase transition in extremely thin Bi film grown on Si(111) substrate. A simple picture to describe this transition process would be the Bi atom inside the A7 primitive cell (green atom in Fig. 2a) moves gradually from the off-center position along the diagonal axis to the center (dashed circle). At the same time, the Rhombohedral cell gradually shifts to a pseudocubic shape. A transition region from pure A7 to A17 phase is expected, which is neither standard A7 nor A17. We can call this region the pseudocubic phase. Here, the spatial extension of the transition region depends on the growth conditions.

To further investigate the influence of this phase transition process on phonon dynamics, we conducted coherent phonon spectroscopic measurements. Degenerate pump-probe experiments were performed in a non-collinear reflection geometry at room temperature with a mode-locked Ti:Sapphire femtosecond laser (Spitfire ACE, Spectra Physics). Both pump and probe pulses have an 800 nm central wavelength, ~258 fs pulse width (FWHM) coming onto the sample surface at a 5 kHz repetition rate. The absorption depth for bismuth at 800 nm is 14.7~15 nm ^{19, 20}. Pump and probe beams were focused onto the sample surface with spot sizes (diameter at the $\frac{1}{\rho^2}$ intensity) of 84 µm and 42 µm respectively. The pump beam was modulated at 585 Hz by a mechanical chopper and the signal from the probe beam was recorded by a lock-in amplifier (model 7265, Signal Recovery). Coherent phonons (CP) have been used extensively to probe material phase change processes, even at ultrafast time scales ²¹⁻²³. Fig. 3 shows the CP signals in all samples under different pump fluences. In our experiment, we only observed A_{1g} mode (see FFT spectrum in Fig. S5). For all fluences, there is a sign change, from positive to negative, of the first peak when the film thickness is below 15 nm. With the transfer matrix method (see Fig. S6) ²⁴, we have found that this sign change is a result of multi-reflection of light wave when the film thickness is comparable with optical penetration depth (~15 nm in Bi at 800 nm). The raw data consists of both CP signals and electronic background, to extract the pure CP signals, we apply a digital band-pass

filter to remove the slowly varying electronic background. Then the CP signals can be fitted with damping harmonic oscillators to obtain CP properties, such as phonon lifetime (τ_p) and phonon frequency (f).

$$\frac{\Delta R}{R} = A \exp(-t/\tau_p) \cos(2\pi(f + \beta t)t + \phi_0) \tag{1}$$

where A, τ_p , f, β and ϕ_0 are the amplitude, dephasing time, initial frequency, the linear chirp rate and initial phase, respectively. For the 4 nm sample, containing no obvious signals, neither electron nor CP oscillations, were observed for the pump fluence up to 1.81 mJ/cm² (Fig. 3c). The signal at higher fluence at 3.98 mJ/cm² is from Si (see Fig. S7) and Bi thin film has been damaged.

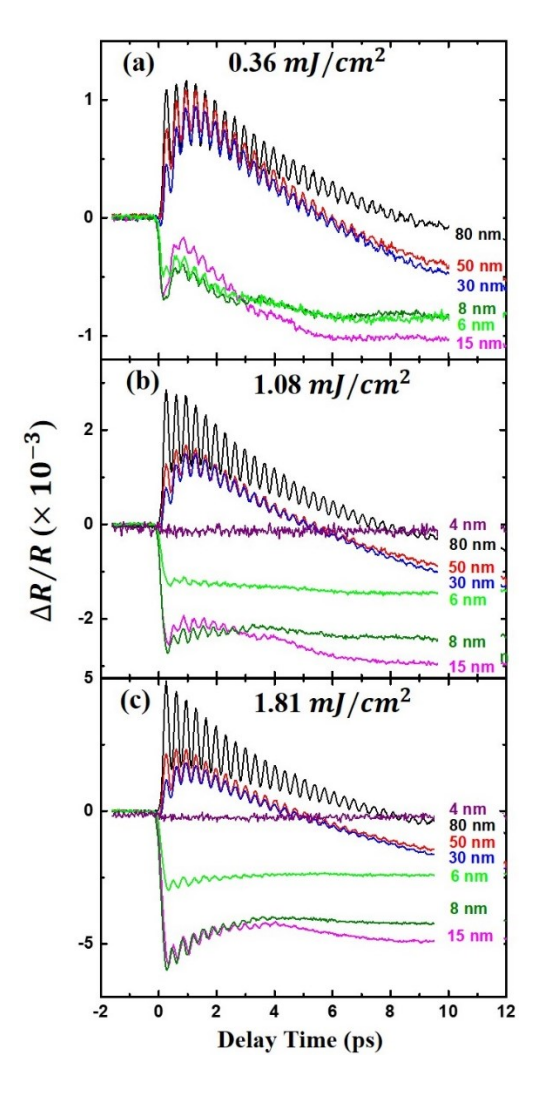


Figure 3 Transient reflectivity change of bismuth thin films on silicon substrate at fluences of 0.36 mJ/cm² (a), 1.08 mJ/cm² (b), and 1.81 mJ/cm² (c).

Fig. 4 presents the CP lifetimes and frequencies as a function of pump fluences, F (Fig. 4 a&b). In Bismuth, it is well accepted that CPs are excited through the DECP process (displace excitation of coherent phonons) 25 . From the extracted phonon frequency and dephasing time, the excited phonon mode is the optical A_{1g} . From the Raman spectra in Fig. 2b, both E_g and A_{1g} phonon modes disappear in 4 nm sample. Consequently, there is no surprise in the disappearance of CP signals in 4 nm sample (Fig. 3c). CP measurements also confirm that there is a complete phase transition in the 4 nm sample. Fig. 4 a&b show that both τ and f decrease with pump fluence in all samples. However, the decreasing trend clearly shows two distinct groups. For samples with thicknesses of 80 nm, 50 nm, and 30 nm, the trends indicating a decrease with pump fluence ($d\tau/dF$, df/dF) are almost the same. For samples of 15 nm, 8 nm and 6 nm, the decreasing trends with fluence are more than 3x faster.

The significant difference between the two groups of samples can be attributed to the phase transition from A7 to A17 structure. Beyond 30 nm, the pump/probe pulses mainly excite/probe the region of pure A7 phase with optical penetration depth $\delta \sim 15$ nm at 800 nm. When the film thickness goes down to a value comparable to δ , the laser pulses start to excite/probe the pseudocubic phase (transition region) and the A17 phase partially. The pure A17 phase could extend up to 4 nm thick, depending on the growth conditions ^{17, 18, 26}. Since the pure A17 phase does not contribute the CP signals, the differences between these two groups could come from the pseudocubic phase. Firstly, the faster decrease of phonon frequency with F indicates stronger bond softening effects. In Fig. 2a, the atom inside the primitive cells moves towards the center in the pseudocubic phase. During this process, the total system energy of the pseudocubic phase should be higher than both the A7 and A17 phases. The potential field of pseudocubic phase has a larger anharmonicity than the A7 and A17 phases, which could be disturbed more easily through the use of an external electromagnetic field. Secondly, faster decrease of τ indicates stronger scattering. In the pseudocubic phase, the phonon frequencies at different thickness are expected to have a continuous change when transitioning from A7 to A17 structures, as they occur gradually. Naturally, this smooth transition would bring more phonon-phonon scattering channels.

Aside from the phase transition relationship driven by film thickness, another possible contribution of the observed phenomenon is a light-driven temporary phase transition. Teitelbaum *et al.* reported a real time observation of a high-symmetry phase in both 20 nm and 275 nm bismuth

films with single-shot pump-probe spectroscopy ¹². When more than 2% of the total valence electrons are excited, where 1% corresponds to a carrier density of 1.43×10²¹ /cm³, it has been proposed that the potential barrier of the A7 structure could become shallower, so much so that Peierls distortion could be temporarily removed ^{12, 27}. A temporary phase transition from A7 to a pseudocubic structure is possible. The main evidence of phase transition in Teitelbaum's work is the fast decrease of phonon frequency with pump fluence and the eventual disappearance of coherent phonon signals. Samples used in Teitelbaum's work were prepared with a sputtering technique on sapphire and glass substrates. Hence all their samples are polycrystalline, having a pure A7 phase where there is no permanent phase transition with thickness. When they extrapolate the fluence dependent phonon frequency to zero pump fluence, the results in both thick and thin samples tend to converge to the same point. It was concluded that the phonon ground state in all of their samples are the same. In our results, we observed a similar phenomenon for samples of 80 nm, 50 nm and 30 nm, signifying these samples share the same phonon ground state. However, in the thin films (especially in 8 nm and 6 nm), the extrapolated phonon frequency at F=0 is higher than that of the thick samples. This indicates that the phonon ground state in these thin films are different from that of the thick films. This also signifies a permanent phase transition with thickness. According to the estimation of the average excited carrier density in our samples ¹⁹, under the fluence of 1.08 m J/cm², the photoexcited carrier densities are 0.5×10^{21} /cm³, 0.7×10^{21} $/\text{cm}^3$, $1.1 \times 10^{21} / \text{cm}^3$, $1.6 \times 10^{21} / \text{cm}^3$, $1.9 \times 10^{21} / \text{cm}^3$ and $2.0 \times 10^{21} / \text{cm}^3$ for 80 nm, 50 nm, 30 nm, 15 nm, 8 nm and 6 nm, respectively. Due to the fact that we used regular pump-probe spectroscopy to excite and detect the coherent phonons, where multiple photons are absorbed, the samples were damaged before the pump fluence reached a threshold to completely remove the potential barrier of Peierls distortion. However, the much faster down-shift of phonon frequency in thinner films (15 nm, 8 nm, 6 nm) with pump fluence indicates that the effect of a shallower potential barrier is much more obvious at these excited carrier densities. Considering the existence of a permanent phase transition region in these thin films, where the potential barrier is already flatter than the pure A7 structure, it is justifiable to recognize the fast decreasing trend of phonon frequency with relation to a relatively low carrier density.

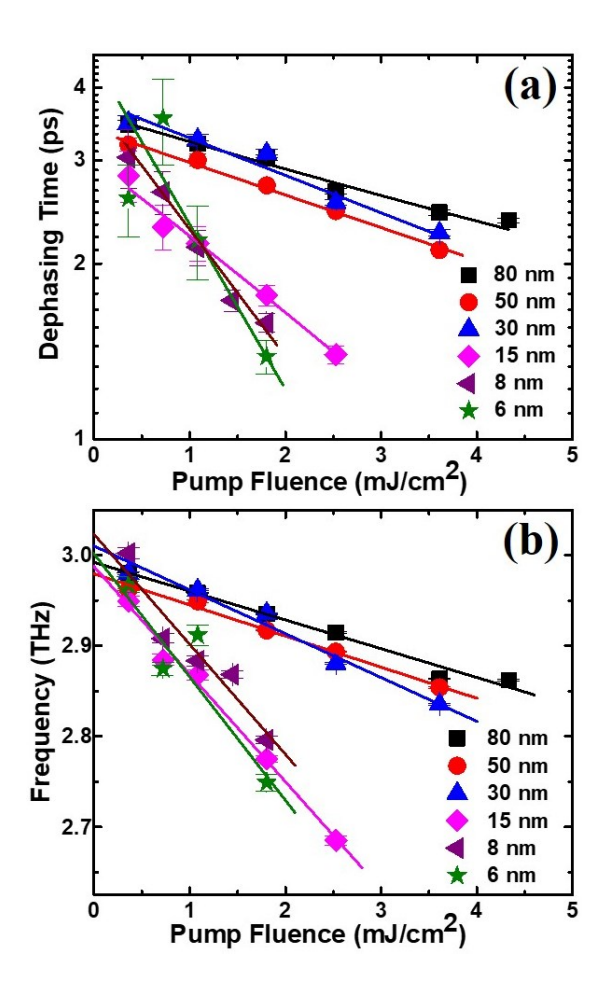


Figure 4 Fluence dependent coherent A_{1g} dephasing time, τ_p , (a) and initial frequency, f, (b) obtained from fitting for different bismuth thicknesses ranging from 6 nm to 80 nm. The solid lines in (a) and (b) are guides to the eye.

In summary, we have demonstrated a layer dependent phase transition from the A7 to the A17 crystal structure in MBE-grown Bi thin films via Raman spectroscopy. Both the A_{1g} and E_{g} phonon modes disappear abruptly in 4 nm thick films, indicating a complete transition to the A17 phase. Ultrafast coherent phonon dynamics bifurcate into two distinct groups: thick (80 nm, 50 nm and 30 nm) and thin (15 nm, 8 nm and 6 nm) samples. Thin samples (\leq 15 nm) exhibited lower phonon frequency and shorter phonon lifetimes than that of the thick samples (\geq 30 nm). We attribute this behavior to two causes: the quasi-cubic phase in the transition region and the temporary phase transition driven by photo-excited carriers. Our results not only provided evidence of a transition to the A17 phase in ultrathin MBE grown Bi film on Si(111) substrate, but also reveal the influence of this phase transition on phonon dynamics. Understanding these

material aspects is imperative to the facilitation of Bi thin film applications in cutting-edge electronic devices.

See supplementary material for the sample information, Transfer Matrix Method and FFT spectrum.

We acknowledge the help of Xianghai Meng with Raman measurements in Jung-fu Lin's laboratory. The authors acknowledge supports from National Science Foundation (NASCENT, Grant No. EEC-1160494; CAREER, Grant No. CBET-1351881; CBET-1707080; Center for Dynamics and Control of Materials DMR-1720595) and Semiconductor Research Corporation and Texas Instruments Fellowships.

The data that supports the findings of this study are available within the article [and its supplementary material].

References

- 1. H. Jones, Proceedings of the Royal Society of London. Series A-Mathematical and Physical Sciences **147**, 396-417 (1934).
- 2. O. Prakash, A. Kumar, A. Thamizhavel and S. Ramakrishnan, Science **355**, 52 (2017).
- 3. D. M. Fritz, D. Reis, B. Adams, R. Akre, J. Arthur, C. Blome, P. Bucksbaum, A. L. Cavalieri, S. Engemann and S. Fahy, Science **315**, 633 (2007).
- 4. H. Du, X. Sun, X. Liu, X. Wu, J. Wang, M. Tian, A. Zhao, Y. Luo, J. Yang and B. Wang, Nat. Commun. 7, 10814 (2016).
- 5. N. Marcano, S. Sangiao, C. Magen, L. Morellón, M. R. Ibarra, M. Plaza, L. Pérez and J. De Teresa, Phys. Rev. B **82**, 125326 (2010).
- 6. N. Armitage, R. Tediosi, F. Lévy, E. Giannini, L. Forro and D. Van Der Marel, Phys. Rev. Lett. **104**, 237401 (2010).
- 7. S. Xiao, D. Wei and X. Jin, Phys. Rev. Lett. **109**, 166805 (2012).
- 8. L. Chen, Z. Wang and F. Liu, Phys. Rev. B **87**, 235420 (2013).

- 9. I. K. Drozdov, A. Alexandradinata, S. Jeon, S. Nadj-Perge, H. Ji, R. J. Cava, B. A. Bernevig and A. Yazdani, Nat. Phys. **10**, 664 (2014).
- 10. C.-H. Hsu, X. Zhou, T.-R. Chang, Q. Ma, N. Gedik, A. Bansil, S.-Y. Xu, H. Lin and L. Fu, Proc. of the Natl. Acad. Sci. 116, 13255-13259 (2019).
- 11. F. Schindler, Z. Wang, M. G. Vergniory, A. M. Cook, A. Murani, S. Sengupta, A. Y. Kasumov, R. Deblock, S. Jeon, I. Drozdov, H. Bouchiat, S. Guéron, A. Yazdani, B. A. Bernevig and T. Neupert, Nat. Phys. **14**, 918-924 (2018).
- 12. S. W. Teitelbaum, T. Shin, J. W. Wolfson, Y.-H. Cheng, I. J. Porter, M. Kandyla and K. A. Nelson, Phys. Rev. X 8, 031081 (2018).
- 13. M. Hase, M. Kitajima, S.-i. Nakashima and K. Mizoguchi, Phys. Rev. Lett. **88**, 067401 (2002).
- 14. S. W. Teitelbaum, T. Henighan, Y. Huang, H. Liu, M. P. Jiang, D. Zhu, M. Chollet, T. Sato, É. D. Murray, S. Fahy, S. O'Mahony, T. P. Bailey, C. Uher, M. Trigo and D. A. Reis, Phys. Rev. Lett. **121**, 125901 (2018).
- 15. J. Toudert and R. Serna, Opt. Mater. Express 7, 2299 (2017).
- 16. A. Fang, C. Adamo, S. Jia, R. J. Cava, S.-C. Wu, C. Felser and A. Kapitulnik, Sci. Adv. 4, eaaq0330 (2018).
- 17. T. Nagao, J. Sadowski, M. Saito, S. Yaginuma, Y. Fujikawa, T. Kogure, T. Ohno, Y. Hasegawa, S. Hasegawa and T. Sakurai, Phys. Rev. Lett. **93**, 105501 (2004).
- 18. S. Yaginuma, T. Nagao, J. Sadowski, M. Saito, K. Nagaoka, Y. Fujikawa, T. Sakurai and T. Nakayama, Surf. Sci. **601**, 3593 (2007).
- 19. T. Shin, J. W. Wolfson, S. W. Teitelbaum, M. Kandyla and K. A. Nelson, Phys. Rev. B **92**, 184302 (2015).

- 20. K. Ishioka, M. Kitajima, O. V. Misochko and T. Nagao, Phys. Rev. B 91, 125431 (2015).
- 21. W. Wu, F. He and Y. Wang, J. Appl. Phys. 119, 055701 (2016).
- 22. M. Först, C. Manzoni, S. Kaiser, Y. Tomioka, Y. Tokura, R. Merlin and A. Cavalleri, Nat. Phys. 7, 854 (2011).
- 23. M. Rini, N. Dean, J. Itatani, Y. Tomioka, Y. Tokura, R. W. Schoenlein and A. Cavalleri, Nature 449, 72 (2007).
- 24. F. He, E. S. Walker, Y. Zhou, S. E. Muschinske, S. R. Bank and Y. Wang, Appl. Phys. Lett. **116** (26), 263101 (2020).
- 25. H. Zeiger, J. Vidal, T. Cheng, E. Ippen, G. Dresselhaus and M. Dresselhaus, Phys. Rev. B 45, 768 (1992).
- 26. E. S. Walker, Phase Transitions, Transfer and Nanoscale Growth of Epitaxial Bi and Bi_{1-x}Sb_x Thin Films, Doctoral dissertation, The University of Texas at Austin, Austin, 2018.
- 27. E. Murray, D. Fritz, J. Wahlstrand, S. Fahy and D. Reis, Phys. Rev. B **72**, 060301 (2005).